Wiley
Journal of Zoological Systematics and Evolutionary Research
Volume 2025, Article ID 9954525, 18 pages
https://doi.org/10.1155/jzs/9954525

WILEY

Research Article

Two New Species of Bipaliinae Land Planarians (Platyhelminthes, Tricladida, Geoplanidae) From the Republic of Korea, Based on an Integrative Taxonomic Approach

Ji-Hun Song[1] **and Fernando Carbayo**[2]

[1]*Animal and Plant Research Division, Nakdonggang National Institute of Biological Resources, Sangju, Republic of Korea*
[2]*Laboratório de Ecologia e Evolução, Escola de Artes, Ciências e Humanidades, Universidade de São Paulo, São Paulo, Brazil*

Correspondence should be addressed to Ji-Hun Song; luckymadang@gmail.com

Received 6 April 2025; Revised 11 July 2025; Accepted 12 July 2025

Academic Editor: Miroslawa Dabert

Land planarians (Platyhelminthes, Geoplanidae) in the Republic of Korea have long been an overlooked taxonomic group, with no formal studies conducted for over a century. Only two species, *Diversibipalium koreense* and *Microplana unilineata*, both described in 1923, have been previously recorded. However, their exact type localities remain uncertain, and no subsequent confirmed records have been reported since their original descriptions, making their current taxonomic status uncertain and in need of reassessment. Here, we present the first taxonomic study of Korean land planarians in over 100 years. By combining morphological and molecular data, we propose two new species of Bipaliinae, *Bipalium gwangneungensis* sp. nov. and *Novibipalium koreanum* sp. nov., collected from multiple administrative regions in the Korean Peninsula. *Bipalium gwangneungensis* sp. nov. is unique for its dorsum color, ranging from beige to gray-beige, a horizontally running unpaired portion of the sperm ducts, a penis papilla located dorsally to the common atrium, and the relative length of the copulatory apparatus, with the portion anterior to the gonopore (male) being 1.4 times as long as the posterior portion (female). Additionally, the female genital canal is elongated and inclined ventroanteriorly toward the gonopore. In contrast, *Novibipalium koreanum* sp. nov. is distinguished by its dorsum, which is ornamented with three or five black longitudinal stripes, a penis bulb located anterior to the penis papilla, and shell glands opening along the proximal, dilated portion of the female genital canal. Phylogenetic analyses of concatenated (18S rDNA, 28S rDNA, and COI mtDNA) and single-gene datasets robustly support the monophyly of each new species, providing strong evidence for the validity of our species delineation. Our study highlights the need for further taxonomic research on this historically overlooked invertebrate group in the Republic of Korea.

Keywords: *Bipalium gwangneungensis* sp. nov; integrative taxonomy; Korean Peninsula; new species; *Novibipalium koreanum* sp. nov; phylogeny

1. Introduction

To date, only two species of land planarians, *Diversibipalium koreense* (Frieb, 1923) and *Microplana unilineata* (Frieb, 1923), have been recorded in the Republic of Korea, indicating that little research has been conducted on land planarians in the country. Moreover, the occurrences and type localities of these two species, collected in 1905 and reported in 1923, remain unclear. Hence, no land planarian species is officially included in the "National List of Species of Korea" [1], published by the government of the Republic of Korea. Further investigation into the type localities of these two species is needed, and additional studies using new specimens should be conducted to formally include them in the "National List of Species of Korea." In 2020, a terrestrial invertebrate sampling campaign conducted by J.-H. Song in the Republic of Korea revealed the presence of diverse morphotypes of land planarians based on field observations, indicating that numerous species may

inhabit the country. In response to these preliminary findings, an international collaborative research initiative was launched in 2021 with the aim of investigating the biodiversity of land planarians in the region and documenting the species present. As part of this initiative, F. Carbayo visited the Republic of Korea in 2022 and, in collaboration with J.-H. Song, carried out a joint field survey. This expedition once again confirmed the occurrence of a variety of land planarian species in the country.

Among the four subfamilies of land planarians (Platyhelminthes, Geoplanidae), only members of Bipaliinae Stimpson, 1857, can be readily identified by their external appearance, as their anterior region is laterally expanded to form a hammer-shaped, half-moon, or sickle-shaped head [2]. This subfamily comprises approximately 192 species, and is subdivided into five genera, namely *Bipalium* Stimpson, 1857 (53 spp.), *Humbertium* Ogren and Sluys, 2001 (25 spp.), *Novibipalium* Kawakatsu, Ogren, and Froehlich, 1998 (8 spp.), *Umbotectum* Solà and Sluys, 2023 (5 spp.), and *Vermiviatum* Solà and Sluys, 2023 (1 sp.), plus the collective genus *Diversibipalium* Kawakatsu, Ogren, Froehlich, Takai, and Sasaki, 2002 (100 spp.), the latter for *species inquerendae* and *nomina dubia* [3].

Bipaliinae is naturally distributed across Madagascar, as well as South, East, and Southeast Asia [4]. A few species, particularly *Bipalium kewense*, are well known for having widely expanded distributional ranges due to human activities [5]. Recently, 14 putative species of Bipaliinae were identified in Korea through molecular analysis of specimens collected on the Korean Peninsula from 2020 to 2022 [6]. Furthermore, in their postscript, they suggested the presence of 20 additional species [6]. In this study, we describe two of the putative species previously identified in that paper, belonging to the genera *Bipalium* and *Novibipalium*. We also provide molecular evidence supporting their monophyly. To our knowledge, this is the first taxonomic description of land planarians from the Republic of Korea in over a century.

2. Materials and Methods

2.1. Sampling and Morphological Study. We conducted sampling in the administrative divisions of Chungcheongbuk-do, Gangwon-do, Gyeonggi-do, and Gyeongsangbuk-do, Republic of Korea (Figure 1). The map showing the collection sites was generated using SimpleMappr [7]. The animals were collected under rocks and rotting logs during the day and on the soil surface at night from 2020 to 2022. We photographed the animals and euthanized them by pouring boiling water over them. Subsequently, we removed a small piece from each animal and preserved it in 100% ethanol, while the main body part was fixed in 100% ethanol or a formaldehyde calcium acetate (FCA) solution that we prepared ourselves for histological studies. The FCA solution was composed of 100 mL of 37% formaldehyde, 17 g of anhydrous calcium acetate, and 900 mL of distilled water. The specimens were cut into a variable number of pieces containing the cephalic, ovarian, prepharyngeal regions, the pharynx, and the copulatory apparatus. These fragments were then dehydrated in a graded ethanol series, cleared in clove oil, and infiltrated and embedded in Paraplast Tissue

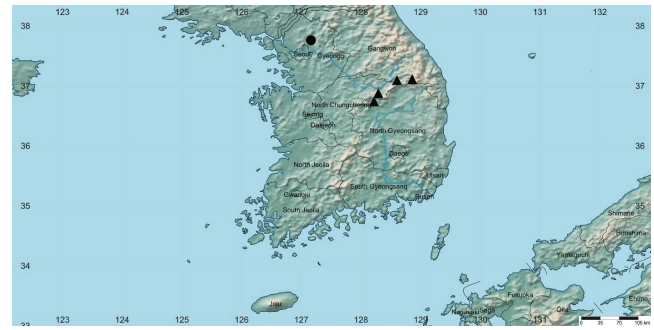

FIGURE 1: Map showing the collection sites of two new species in the Republic of Korea. Black-filled circles indicate *Bipalium gwangneungensis* sp. nov., whereas black-filled triangles denote *Novibipalium koreanum* sp. nov.

Embedding Medium. We sectioned these tissue blocks at 7 μm intervals using a retracting rotary microtome, affixed with albumin–glycerol (1:1) on glass slides placed on a slide warmer, stained them with the Mallory–Heidenhain method modified by Cason [8], dehydrated them in a graded ethanol series, cleared them in xylene, and mounted them in Entellan or Synth mounting media. We examined the slides with an optical microscope and made drawings of the copulatory apparatus with a camera lucida attached to the microscope. We named the colors of the bodies of living and fixed specimens according to the RAL color palette (RAL gemeinnützige GmbH, available at https://www.ral-farben.de/uebersicht-ral-classic-farben.html?&L=1, last accessed in September 2023) by comparing digital images of the specimens on a computer screen. The thickness of the cutaneous musculature relative to body height was calculated from the prepharyngeal region, following Froehlich [9]. The same procedure was applied to the parenchymatic musculature thickness, following Winsor [5]. The type specimens were deposited in the Nakdonggang National Institute of Biological Resources (NNIBR), Republic of Korea.

2.2. DNA Extraction, PCR Amplification, and Sequencing. Genomic DNA was extracted from tissues (~2 mm in length) from the posteriormost region of the body, using the QIAGEN DNeasy Blood and Tissue Kit (Qiagen, Hilden, Germany) according to the manufacturer's instructions. The remainder of the body was preserved in 80% ethanol for further morphological analysis. PCR amplification and sequencing were performed with the primer sets described in Table 1. Purification and sequencing of PCR products were carried out by Macrogen Corporation (Daejeon, Republic of Korea).

2.3. Phylogenetic Analysis. All sequences were aligned using the MAFFT align option with default parameters in Geneious Prime v.2019.0.4 [14]. Four different datasets were generated, including GenBank sequences and new sequences from Korean specimens, and used them for the phylogenetic inference (Table 2). Dataset 1 (5023 bp) was a concatenated set containing 18S rDNA (1774 bp), 28S rDNA (1686 bp), and COI mtDNA (1563 bp). Datasets 2–4, which were single-gene datasets, correspond to 18S rDNA (1781 bp), 28S rDNA (1691 bp), and COI mtDNA (1563) sequences of the subfamily

Table 1: Primers used to amplify and sequence the DNA fragments.

Target locus	Primer name (direction)	Primer sequence (5′-3′)	Reference
COI	BarS (forward)	GTTATGCCTGTAATGATTG	Álvarez-Presas et al. [10]
	FlatwormCOI-R (reverse)	GAGCAACAACATAATAAGTATCATG	Sunnucks et al. [11]
18S rDNA	1F (forward)	TACCTGGTTGATCCTGCCAGTAG	Carranza et al. [12]
	5R (reverse)	CTTGGCAAATGCTTTCGC	Carranza et al. [12]
	4F (forward)	CCAGCAGCCGCGCTAATTC	Carranza et al. [12]
	9R (reverse)	GATCCTTCCGCAGGTTCACCTAC	Carranza et al. [12]
28S rDNA	28S_1F (forward)	TATCAGTAAGCGGAGGAAAAG	Álvarez-Presas et al. [13]
	28S_4R (reverse)	CCAGCTATCCTGAGGG	Álvarez-Presas et al. [13]
	28S_2F (forward)	CTGAGTCCGATAGCAAACAAG	Álvarez-Presas et al. [13]
	28S_6R (reverse)	GGAACCCCTTCTCCACTTCAGT	Álvarez-Presas et al. [13]

Table 2: GenBank accession numbers of the specimens used in the phylogenetic analyses of this study.

Species	GenBank accession numbers		
	18S	28S	COI
Bipalium admarginatum	OQ308840	—	NC_072986
Bipalium adventitium	DQ666000	DQ665956	MZ561467
Bipalium gwangneungensis sp. nov.	PQ652198	PQ652205	PQ653970
Bipalium gwangneungensis sp. nov.	PQ652199	PQ652206	PQ653971
Bipalium gwangneungensis sp. nov.	PQ652200	PQ652207	PQ653972
Bipalium kewense	OQ859548	OQ859179	NC_045216
Bipalium nobile	DQ666001	DQ665958	MG436935
Bipalium rhytidoantrum	OQ859546	OQ859177	OQ849802
Bipalium rugiantrum	OQ859547	OQ859178	OQ849803
Bipalium vagum	MZ520992	MZ520985	MZ561468
Diversibipalium castaneum	OQ859551	OQ859183	OQ849808
Diversibipalium contortolineatum	OQ859553	OQ859186	—
Diversibipalium duplalaticlavium	OQ859552	OQ859185	—
Diversibipalium marginatanigrum	OQ859550	OQ859182	OQ849807
Diversibipalium mayottensis	MZ520997	MZ520986	MZ561470
Diversibipalium multilineatum	MZ520994	MZ520987	MZ561469
Humbertium ithorense	OQ859549	OQ859181	OQ849806
Novibipalium koreanum sp. nov.	PQ652201	PQ652208	PQ653973
Novibipalium koreanum sp. nov.	PQ652202	PQ652209	PQ653974
Novibipalium koreanum sp. nov.	PQ652203	PQ652210	PQ653975
Novibipalium koreanum sp. nov.	PQ652204	PQ652211	PQ653976
Novibipalium rhynchophorum	OQ859556	OQ859176	—
Novibipalium venosum	DQ666019	DQ665981	DQ666048
Umbotectum capitofalcatum	OQ859558	OQ859184	OQ849809
Vermiviatum covidum	MZ520996	MZ520989	MZ561471
Vermiviatum covidum	MZ520995	MZ520988	MZ561472
Outgroup			
Microplana henrici	KU872590	KU872628	KU867165
Microplana terrestris	KU872613	KU872657	KU867226

Note: The sequences of *Bipalium gwangneungensis* sp. nov. and *Novibipalium koreanum* sp. nov. were generated in this study.

Bipaliinae, respectively. In all four data sets, the outgroup from the subfamily Microplaninae was used.

Maximum likelihood (ML) analysis and dataset-specific model selection were assessed on the W-IQTREE web server (http://iqtree.cibiv.univie.ac.at/) [15]. The models selected for each dataset were HKY + F + I + G4 (18S rDNA partition), TVM + F + I + G4 (28S rDNA partition), GTR + F + I + G4 (COI mtDNA partition) (dataset 1, concatenated); TPM2u + F + I + G4 (dataset 2, 18S rDNA); TVM + F + I + G4 (dataset 3, 28S rDNA); and GTR + F + I + G4 (dataset 4, COI mtDNA).

Figure 2: *Bipalium gwangneungensis* sp. nov. Photographs of living (A, B) and preserved (C, D) paratypes. A NNIBRIV93457. B NNIBRIV93457 and NNIBRIV95892 during mating. (C, D) NNIBRIV95892 in dorsal (C) and ventral (D) views. Scale bars: 10 mm. go, gonopore; px, pharynx.

Branch support in the ML analysis was performed with 1000 ultrafast bootstrap (UFBoot) replicates, and the SH-aLRT test was also performed [16]. A clade is considered highly supported if its SH-aLRT is greater than 80% and its UFBoot value is greater than 95% [17]. Phylogenetic trees were constructed and visualized using iTOL v6 [18].

3. Results

3.1. Systematic Account. Family Geoplanidae Stimpson, 1857

New Korean name (not a direct translation, but a newly coined name derived from the etymology or ecology of the taxon) for the family Geoplanidae: "Seup-ji-peul-la-na-ri-a-gwa," denoting a family of planarians that inhabit moist land.

Subfamily Bipaliinae Stimpson, 1857

New Korean name for the subfamily Bipaliinae: "Mang-to-meo-ri-peul-la-na-ri-a-a-gwa," denoting a subfamily within the family Geoplanidae with a cloak-shaped head.

Genus *Bipalium* Stimpson, 1857

New Korean name for the genus *Bipalium*: "Mang-to-meo-ri-peul-la-na-ri-a-sok," denoting a genus within the subfamily Bipaliinae with a cloak-shaped head.

Bipalium gwangneungensis sp. nov.

New Korean name for the new species: "Gwang-neung-mang-to-meo-ri-peul-la-na-ri-a," denoting a newly discovered species within the genus *Bipalium* with a cloak-shaped head that inhabits Gwangneung

(Figures 2–6).

Zoobank registration: LSID: urn:lsid:zoobank.org:act:E8242AF9-B013-49FF-8C9E-925C9F6FEB85

Etymology. The specific epithet is derived from the type locality (Gwangneung Forest, UNESCO Biosphere Reserve) of the new species.

Diagnosis. *Bipalium* species with the dorsum color ranging between beige and gray beige; preserved body 22–42.5 mm in length; unpaired portion of the sperm ducts runs horizontally; prostatic vesicle elongated, oriented horizontally; penis papilla dorsal to the common atrium; relative length of the portion of the copulatory apparatus anterior to the gonopore (male) 1.4 times longer than the female portion; female genital canal elongated and inclined ventroanteriorly toward the gonopore; openings of the male atrium and female genital canal dorsal to the gonopore; common atrium expanded.

Material examined. All type specimens were collected in Gwangneung Forest (Korea National Arboretum); 415, Gwangneungsumogwon-ro, Soheul-eup, Pocheon-si, Gyeonggi-do, Republic of Korea; 37°45′33″N, 127°09′41″E; June 10, 2022; coll. J.-H. Song, Y. H. Lee and K. A. Kim. *Holotype*: NNIBRIV93458 (Field code, 241_1): Sagittal sections of the copulatory apparatus on 12 slides. *Paratypes*: NNIBRIV95892 (Field code, 240_4): Transverse sections of the cephalic extremity on eight slides; horizontal sections of a region behind head on seven slides; transverse sections of the prepharyngeal region on five slides; sagittal sections of the pharynx and copulatory apparatus on 48 slides. NNIBRIV93456 (Field code, 240_1): Transverse-to-horizontal

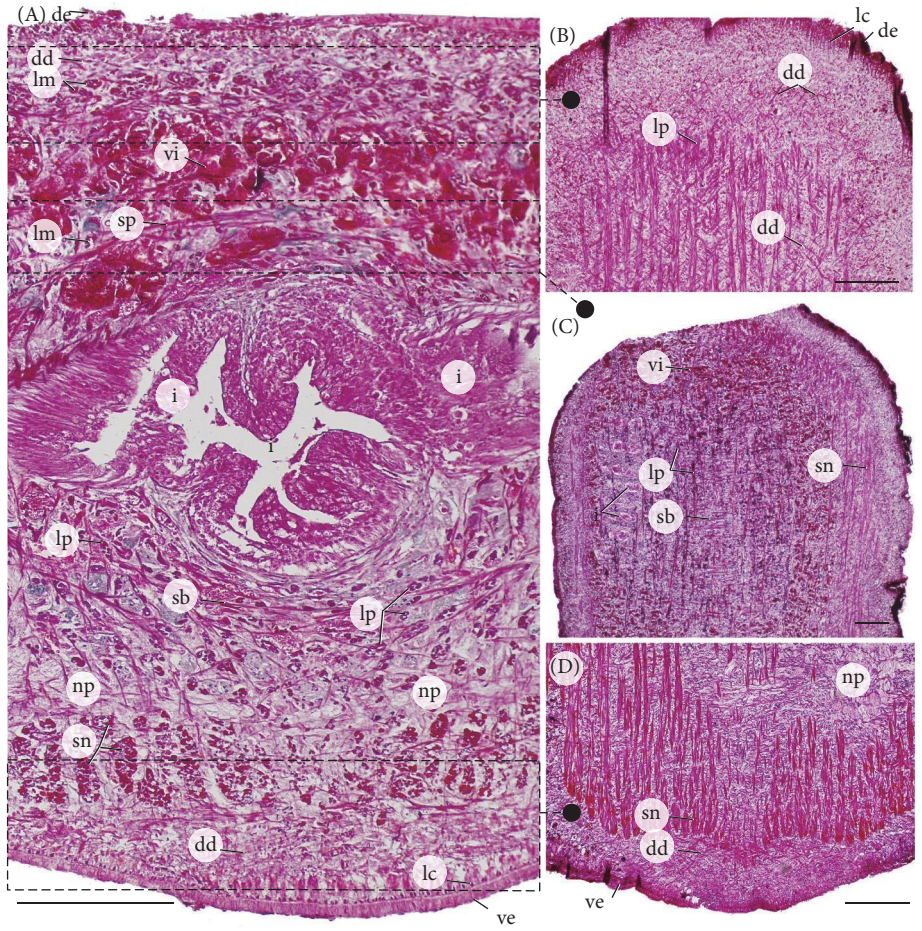

Figure 3: Photomicrographs of *Bipalium gwangneungensis* sp. nov. (A) transverse section of the prepharyngeal region of paratype NNIBRIV93456. (B–D) Horizontal sections of the supraintestinal (B), subintestinal (C), and subneural (D) regions of the paratype NNIBRIV95892 showing the parenchymal musculature at levels approximately equivalent to those marked with dashed lines in A. Scale bars: 250 μm. dd, diagonal parenchymatic muscle; de, dorsal epidermis; i, intestine; lc, longitudinal cutaneous muscle; lm, longitudinal muscles; lp, longitudinal parenchymal muscle; np, nerve plate; sb, subintestinal transverse parenchymal muscles; sn, subneural parenchymal muscle of longitudinal fibers; sp, supraintestinal transverse parenchymal muscles; ve, ventral epidermis; vi, vitellaria.

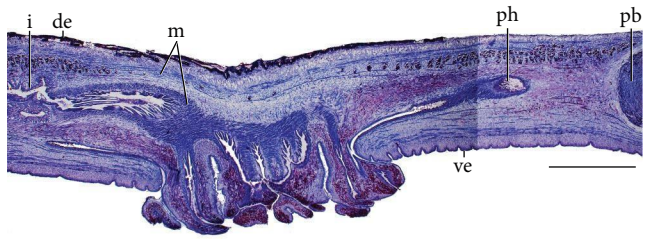

Figure 4: *Bipalium gwangneungensis* sp. nov. Sagittal section of the pharynx protruded through the mouth of the paratype NNIBRIV95892. Scale bar: 1 mm. de, dorsal epidermis; i, intestine; m, muscle; pb, penis bulb; ph, pharyngeal pouch; ve, ventral epidermis.

sections of the cephalic extremity on four slides; transverse sections of prepharyngeal region on 16 slides; sagittal sections of the pharynx on 15 slides; sagittal sections of the copulatory apparatus on 12 slides. NNIBRIV93457 (Field code, 240_5); preserved in 80% ethanol.

Distribution. Only known from the type locality.

Type locality. Gwangneung Forest (KNA: Korea National Arboretum). Pocheon-si, Gyeonggi-do, Republic of Korea. This forest has been strictly protected since the early 20th century and was designated as a UNESCO Biosphere Reserve in 2010. It is characterized by predominantly native temperate broadleaf vegetation and minimal human disturbance, although a small number of naturalized alien plant species have occasionally been recorded [19].

Description (external). Living animals are elongate, with a laterally expanded cloak-shaped headplate (Figure 2). The sides of the head are rounded, not recurved at its maximum width, which is 1.4 times that of the body. The preserved adults

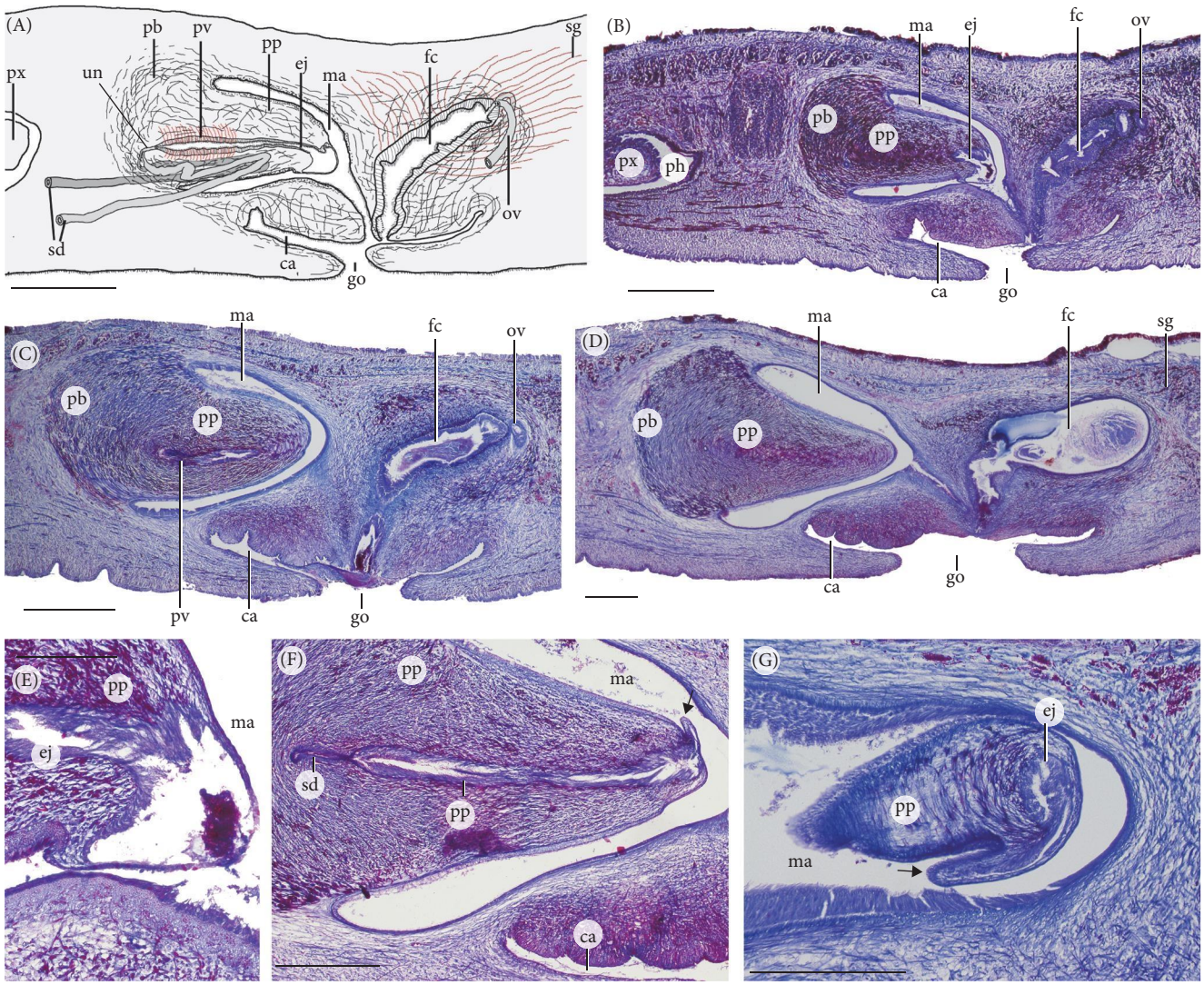

FIGURE 5: *Bipalium gwangneungensis* sp. nov. Diagrammatic reconstruction (A) and sagittal sections of the copulatory apparatus (A–G) of the holotype (A, B, E), and the paratypes NNIBRIV95892 (D, F) and NNIBRIV93456 (G). Arrows point to the thin tip of the penis papilla. Scale bars: 500 μm (A–D, F–G) and 100 μm (E). ca, common genial atrium; ej, ejaculatory duct; fc, female genital canal; go, gonopore; ma, male genital atrium; ov, ovovitelline duct; pb, penis bulb; ph, pharyngeal pouch; pp, penis papilla; pv, prostatic vesicle; px, pharynx; sd, sperm duct; sg, shell glands; un, unpaired sperm duct.

measured 22.0–42.5 mm in length, with the body width: length ratio 1:8.5–1:15.9. The mouth of the preserved specimens laid at a distance from the anterior end equivalent to 52% of the body length, and the gonopore at 68%.

The dorsal side of the living specimens ranges between beige (RAL 1001) and gray beige (RAL 1019), with lighter margins. The cephalic region is brown gray (RAL 7013; Figure 2A,B). The color of the ventral side in life was not documented. The dorsal side of the preserved specimens becomes sand yellow (RAL 1002) (Figure 2C), while that of the ventral side is oyster white (RAL 1013) (Figure 2D).

Description (internal). The numerous eyes are 20–25 μm in diameter, and single cup-shaped. They are surround the dorsomarginal surface of the cephalic region. Three-to-four eyes are in a same transverse plane in the mid headplate. Behind the cephalic region the eyes are sparsely distributed along the body margins.

Sensory pits are simple invaginations 32–36 μm deep, situated ventromarginally in a single row which contours the body margin approximately over the anterior half of the headplate.

The width of the creeping sole is 30% the body width. The epidermal cells in the prepharyngeal region, except for the creeping sole, produce rhammites. Some gland cells producing erythrophil granules penetrate the dorsal and ventral epidermis outside the creeping sole. Scarce gland cells producing xanthophil granules penetrate the body margins, while cells producing cyanophil granules penetrate the epithelium of the creeping sole.

The main nervous system consists of a pair of longitudinal nerve cords that expand in the cephalic region to form the cerebral ganglia. These ganglia are situated 6.6% of the body length from the anterior tip.

The dorsal cutaneous musculature consists of a subepithelial layer of very scattered circular fibers, followed by a one-

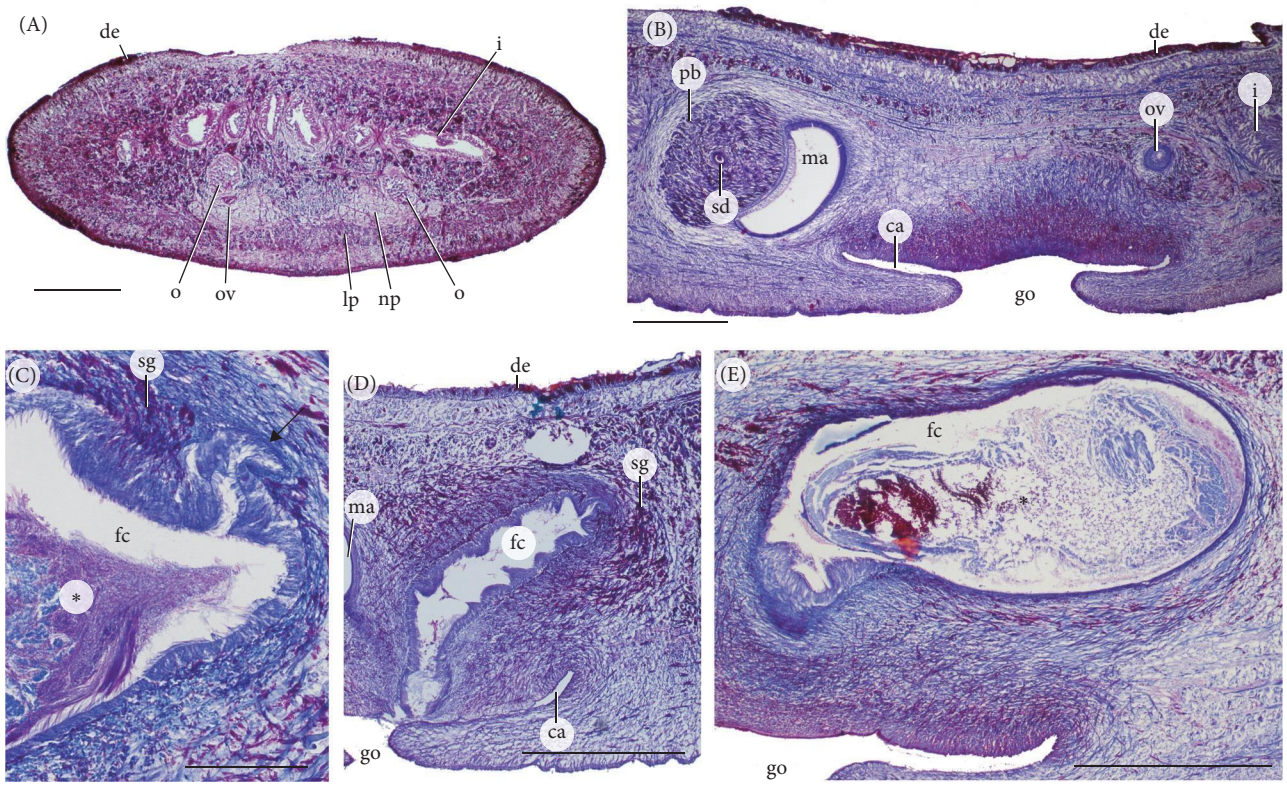

FIGURE 6: *Bipalium gwangneungensis* sp. nov. Transverse (A), parasagittal (A, B) and sagittal (C–E) sections of the copulatory apparatus of the paratypes NNIBRIV95892 (A), NNIBRIV93456 (C), NNIBRIV95892 (B, E) and holotype (D). Scale bars: 500 μm (A, B, D, E) and 100 μm (C). Note region of female genital duct receiving the ovovitelline ducts (arrow) and ejaculate in the female genital duct (asterisk). Scale bars: 500 μm (A–B, D–E) and 100 μm (C). ca, common genial atrium; de, dorsal epidermis; fc, female genital canal; go, gonopore; i, intestine; lp, longitudinal parenchymal muscle; ma, male genital atrium; np, nerve plate; ov, ovovitelline duct; pb, penis bulb; sd, sperm duct; sg, shell glands.

fiber-thick layer of decussate diagonal fibers, and an innermost longitudinal muscle layer made up of small bundles containing two–six fibers each. The ventral cutaneous musculature follows the same pattern as the dorsal, except that the bundles of longitudinal ventral muscles consist of one–three fibers each (Figure 3A). CMI (cutaneous muscle index), 2%.

The parenchymal musculature consists of a dorsal layer of decussate fibers (25–20 μm thick), followed by a strong longitudinal muscle layer with bundles of 7–26 fibers each (Figure 3A–D). The outer bundles of this longitudinal muscle are interwoven with diagonal decussate fibers, while the innermost bundles are interwoven with fibers of the supraintestinal transverse muscle (39–60 μm thick). The subintestinal muscle (40 μm) is composed of transverse fibers mixed with longitudinal muscle bundles (Figure 3A,C). This longitudinal muscle extends to the level of the nerve cords as single fibers. Below the nerve cords is a very strong subneural muscle (100–150 μm thick) composed of longitudinal bundles, each containing 20–65 fibers (Figure 3A,C, D). This longitudinal muscle also extends laterally to join the dorsal longitudinal muscle, forming a muscular tube. Dorsoventral fibers run between the intestinal diverticula. Over the creeping sole, there is a diagonal muscle layer of decussate fibers situated on the inner side of the peripheral nerve plexus and mixed with longitudinal muscle fibers (Figure 3A,D). Some longitudinal muscle fibers are also present above the creeping sole. The PMI (parenchymal muscle index) ranges from 16% to 21%.

The mouth opens approximately in the middle of the pharyngeal pouch. The pharynx is collar-shaped (Figure 4). The outer epithelium of the pharynx is underlain by a one-fiber-thick longitudinal muscle, followed by a 3–6 μm thick circular muscle. The inner pharyngeal epithelium is supported by an 8–10 μm thick longitudinal muscle (50–90 μm thick) followed by an 80–100 μm thick circular muscle.

The testes are located ventrally, immediately above the main nerve system, and are arranged in a single row on each side of the body. The anteriormost testes are situated behind the ovaries, at a distance from the anterior extremity of the body equivalent to 13% of the body length, while the posteriormost testes are located at 43.5% of the body length. The sperm ducts run laterally to the ovovitelline ducts. The distal portion of the sperm ducts is dilated, containing sperm and erythrophil granules. The distal portion of the sperm ducts bends anteriorly, laterally to the male atrium, to penetrate the anteroventral aspect of the penis bulb, which is mostly located anterior to the penis papilla. Subsequently, the sperm ducts bend posteriorly and join into an unpaired common sperm duct. Both the paired and unpaired sperm ducts are lined with a cuboidal, ciliated epithelium. The unpaired duct is surrounded by a 4 μm thick layer of crisscrossed muscle fibers.

This unpaired duct communicates with the anterior portion of the canalicular, intrabulbar prostatic vesicle. The prostatic vesicle is horizontal and connects to the ejaculatory duct, which forms a horizontal canal. The ejaculatory duct dilates at the tip of the penis papilla, forming an irregular-shaped ejaculatory cavity with a minute opening to the male atrium (Figure 5A–G). The horizontal penis papilla is approximately cylindrical, with conical point, with its tip housing a dilation that may be very pointed (Figure 5E–G). This papilla occupies most of the male atrium. The male atrium is not folded, and its anterior two-thirds conform to the shape of the penis papilla, while the distal third forms a canal running ventroposteriorly to open into the common atrium (Figure 5).

The prostatic vesicle is lined with a cuboidal-to-columnar ciliated epithelium, which is penetrated by numerous gland cells producing erythrophil granules. The vesicle is surrounded by a 10–15 μm thick layer of crisscrossed muscle fibers. The ejaculatory duct is lined with cuboidal epithelium proximally and columnar epithelium distally; short cilia were observed scattered along the epithelium, which is underlain by some criss-crossed muscle fibers. The ejaculatory cavity is lined with a squamous epithelium that appears to be so closely attached to the epithelium of the penis papilla that there is no space between both epithelia (Figure 5E). The aperture of this cavity into the male atrium was observed only in the paratypes NNIBRIV95892 and NNIBRIV93456 (Figure 5F,G).

In its proximal section, the penis papilla is lined with a cuboidal epithelium, which transitions to squamous epithelium toward the tip of the papilla. Cilia are present in the epithelium near the insertions of the penis papilla. Gland cells discharge fine erythrophil granules through the papilla's epithelium. The latter is underlain by a circular muscle, up to 10 μm thick in the subapical region, followed by a 3 μm thick longitudinal muscle.

The male atrium is lined with cuboidal epithelium, with cilia present in the dorsal region containing the penis papilla and the canalicular portion. Some gland cells discharge erythrophil granules through the atrial epithelium, which is underlain by a 12 μm thick circular muscle, followed by a 4 μm thick longitudinal muscle. This musculature becomes less prominent in the distal region of the male atrium.

The ovaries are ovoid to quadrangular and measure 250 μm in diameter (Figure 6A). They lie immediately above the ventral nerve cords, located dorsally to the cerebral ganglia at a distance from the anterior end of the body equal to 6.6% of the body length. The vitellaria are distributed around the intestine and between the main intestinal branches (Figure 3A). The ovovitelline ducts emerge from the ventral side of the ovaries. These ducts ascend at the level of the gonopore, and their distal portion bends anteriorly to open almost together into the posterior or posterodorsal portion of the female genital canal (Figures 5A and 6B). The ducts are underlain by a 10 μm thick layer of circular to crisscrossed muscle fibers. The female genital canal is an elongated cavity (Figures 5A–D and 6C–E) that is dilated and horizontal in paratype NNIBRIV95892 (Figure 6E), which was found mating and fixed about 4 h after the mating was interrupted during collection. The proximal two-thirds of the female genital canal runs ventroanteriorly, and the distal third runs almost vertically, opening slightly lateral to the male atrium's entrance into the common atrium (Figures 5A–D and 6D). This canal is lined with a columnar, ciliated epithelium (Figure 6C,D), and its proximal two-thirds is pierced by shell glands. The canal is surrounded by a loose layer of crisscrossed muscle fibers, which become radial and longitudinal in the narrowed portion.

The gonopore is located midway along the common atrium (Figure 5A–D). The position of the gonopore, in relation to the total length of the copulatory apparatus, divides the apparatus into two sections, with the anterior (male) section being 1.4 times as long as the posterior (female) section. The common atrium is flattened dorsoventrally, relatively long, and located below the male and female atria. It is lined with squamous epithelium, which transitions to cuboidal around the gonopore. Cilia are present in the portion anterior to the gonopore, and are particularly conspicuous in the ventral portion. Abundant gland cells discharge erythrophil granules through the dorsal epithelium, which is surrounded by longitudinal and radial muscle fibers. This musculature is situated 15 μm from the epithelium. Scattered cells discharge cyanophil granules through the ventral epithelium, which is underlain by scattered muscle fibers without apparent organization.

Biological note. Paratypes NNIBRIV95892 and NNIBRIV93457 were found during mating and fixed about 4 h after interruption of the copulation.

Comparative discussion. Among the 53 species of *Bipalium*, only nine share two distinctive features with the new species; the relative length of the portion anterior to the gonopore (male), which is between 1.0 and 1.8 times as long as the portion posterior to it (female), and the female genital canal, which is elongated and inclined ventroanteriorly toward the gonopore (Table 3).

These nine species are *Bipalium distinguendum* Müller, 1907; *Bipalium glaucum* (Kaburaki, 1922); *Bipalium kisoense* Kaburaki, 1922; *Bipalium kraepelini* (Ritter-Zahony, 1905); *Bipalium monolineatum* Kaburaki, 1922; *Bipalium muninense* Kawakatsu, Sluys and Ogren, 2005; *Bipalium robiginosum* Graff, 1899; *Bipalium semperi* (Graff, 1899); and *Bipalium sudzukii* Kawakatsu, 1987. Among them, *B. distinguendum*, *B. glaucum*, and *B. robiginosum* differ from the new species in that the openings of the male atrium and female genital canal are posterior to the gonopore (*B. distinguendum* and *B. glaucum*) or anterior to it (*B. robiginosum*), whereas in the new species, the openings are dorsal to the gonopore. Among the remaining six species, only *B. kisoense*, *B. monolineatum*, and *B. semperi* have an elongated prostatic vesicle similar to that of the new species. However, the conical penis papilla is oriented dorsoposteriorly (*B. kisoense*, *B. semperi*) or ventroposteriorly (*B. monolineatum*), but not horizontal as in the new species. Furthermore, the common atrium is very narrow in *B. semperi* (vs. expanded in the new species), whereas the penis papilla is located anterior to the common atrium in *B. kisoense* (vs. dorsal in the new species), and the unpaired portion of the sperm ducts runs vertically in *B. monolineatum* (vs. horizontally in the new species).

Four *Bipalium* species could not be discussed above because the relative position of the gonopore along the copulatory apparatus was not provided in the original descriptions

Table 3: Comparison between *Bipalium gwangneungensis* sp. nov. and species of the genus having a ratio length male copulatory apparatus:female copulatory apparatus ranging between 1:1 and 1.8:1.

Species	Ratio of male:female copulatory apparatus	Female genital canal elongate and ventroanteriorly inclined	Openings of male atrium and female genital canal dorsal to gonopore	Prostatic vesicle elongate	Penis papilla cylindrical	Penis papilla horizontal
Bipalium glandiantrum	1.3:1	No (anterior half pleated)	Yes	No (dilated)	No (conical)	Yes
Bipalium simrothi	1.1:1	No (curved)	Yes	No (dilated)	Yes	No (curved)
Bipalium admarginatum	1.8:1	No (horizontal)	Yes	No (dilated)	No (conical)	Yes
Bipalium crassatrium	1.6:1	No (horizontal)	No (posterior)	Yes	Yes (and minute)	Yes
Bipalium poiense	1.2:1	No (horizontal)	No (posterior)	No (dilated)	Yes	Yes
Bipalium rigaudi-Form 2 (specimens studied by de Beauchamp [20])	1.8:1	No (horizontal)	Yes	Yes	No (conical)	Yes
Bipalium gestroi	1.5:1	No (vertical)	Yes	No (dilated)	No (conical)	Yes
Bipalium distinguendum	1.4:1	Yes	No (posterior)	Yes	No (conical)	No (curved)
Bipalium glaucum	1.4:1	Yes	No (posterior)	Yes	No (conical)	No (curved)
Bipalium robiginosum	1.7:1	Yes	No (anterior)	No (dilated)	No (conical)	Yes
Bipalium kraepelini	1.4:1	Yes	Yes	No (dilated)	No (conical)	No (inclined ventroposteriorly)
Bipalium muninense	1.8:1	Yes	Yes	No (dilated)	No (conical)	Yes
Bipalium sudzukii	1.4:1	Yes	Yes	No (dilated)	No (conical)	Yes
Bipalium semperi	1.1:1	Yes	Yes	Yes	No (conical)	No (inclined ventroposteriorly)
Bipalium kisoense	1.8:1	Yes	Yes	Yes	No (conical)	No (inclined dorsoposteriorly)
Bipalium monolineatum	1.0:1	Yes	Yes	Yes	No (conical)	No (inclined dorsoposteriorly)
Bipalium gwangneungensis sp. nov.	1.4:1	Yes	Yes	Yes	Yes	Yes

FIGURE 7: *Novibipalium koreanum* sp. nov. Photographs of living (A, B) and preserved (C, D, F–H in ethanol, E in clove oil) paratypes NNIBRIV95889 (A), NNIBRIV95888 (B, G), holotype (C–D), and NNIBRIV93444 (E–F) in dorsal (A–C, E, G) and ventral (D, F, H) views. Scale bars: 5 mm. e, eye; go, gonopore; mo, mouth. Arrows point to the arrowhead-shaped glandular zone.

(namely, *Bipalium alternans* de Beauchamp, 1930, *Bipalium dubium* Loman, 1890, and *Bipalium chhatarpurensis* Chaurasia, 1988) or because the work in which the species was described (*Bipalium somii* Chaurasia, 1981, from India) was not available to us. However, the three former species can readily be distinguished from the new species in that *B. alternans* exhibits transverse bands on the dorsum, whereas *B. dubium* displays longitudinal stripes and *B. chhatarpurensis* presents a body with white and black colors. Furthermore, the penis papilla of *B. dubium* is anterior to the common atrium, whereas it is dorsal in the new species.

Genus *Novibipalium* Kawakatsu, Ogren & Froehlich, 1998

New Korean name for the genus *Novibipalium*: "Sae-mang-to-meo-ri-peul-la-na-ri-a-sok," denoting a "newly recognized (*Novi-*, from Latin *novus*)" genus within the subfamily Bipaliinae with a cloak-shaped head.

Novibipalium koreanum sp. nov.

New Korean name for the new species: "Han-guk-sae-mang-to-meo-ri-peul-la-na-ri-a," denoting a newly discovered species within the genus *Novibipalium* with a cloak-shaped head found in the Republic of Korea (Hanguk) (Figures 7–11).

Zoobank registration: LSID: urn:lsid:zoobank.org:act:BAF2EE11-A220-4938-B927-AC97186AC024

Etymology. The specific epithet is derived from the name of the country (Republic of Korea) where the specimens were collected.

Diagnosis. Species of *Novibipalium* have three or five black dorsal longitudinal stripes on a gray background; the sperm ducts run ventrally to the penis papilla; the penis bulb is anterior to the penis papilla; shell glands open along the proximal, dilated portion of the female genital canal, which is approximately 45° inclined toward the gonopore.

Material examined. Holotype: NNIBRIV93445 (Field code, 204_2). 815, Seonamgyegok-ro, Danseong-myeon, Danyang-gun, Chungcheongbuk-do, Republic of Korea; 36°52′31″N, 128°17′26″E; October 22, 2021; coll. J.-H. Song and J. Y. Kim. Sagittal sections of the cephalic extremity on 16 slides; transverse sections of the prepharyngeal region on seven slides; sagittal sections of the pharynx and copulatory apparatus on 41 slides. Paratypes: NNIBRIV93446 (Field code, 204_3): same collection locality and date as holotype; horizontal sections of the cephalic extremity on eight slides; horizontal sections of a body portion behind the head on 12 slides; sagittal sections of the pharynx on 16 slides; sagittal sections of the copulatory apparatus on 15 slides. NNIBRIV93444 (Field code, 76_12): 425, Gimyong-gil, Sanbuk-myeon, Mungyeong-si, Gyeongsangbuk-do, Republic of Korea; 36°44′23″N, 128°13′08″E; June 18, 2020; coll. J.-H. Song and J. Y. Kim; transverse sections of the cephalic extremity on 11 slides; horizontal

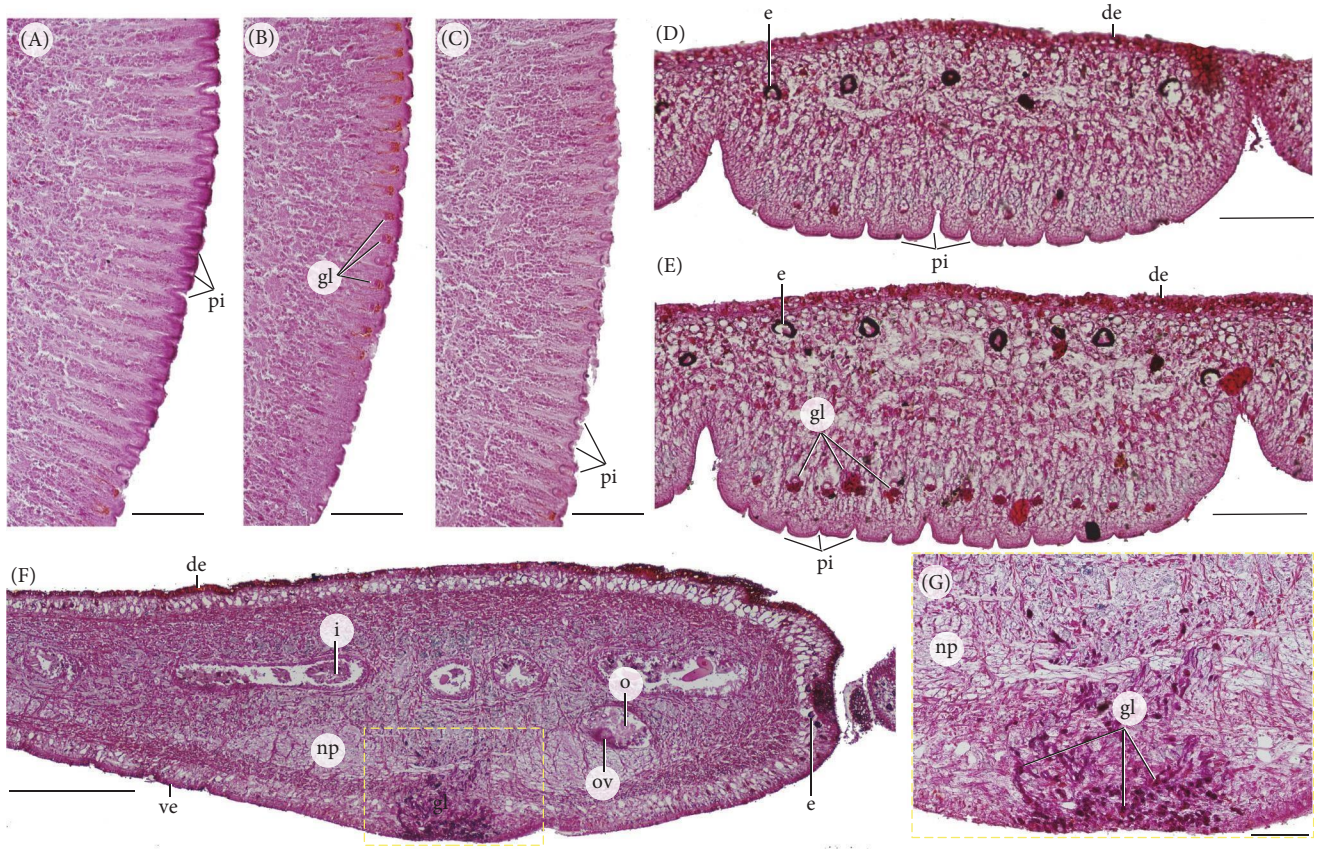

FIGURE 8: *Novibipalium koreanum* sp. nov. Photomicrographs of horizontal (A–C, paratype NNIBRIV95888) and transverse (C–G, paratype NNIBRIV93444) sections of the headplate showing sensory pits and gland cells opening through the ventral arrowhead-shaped zone. The dashed rectangle in F is enlarged in G. Scale bars: 100 μm (A–E, G) and 500 μm (F). de, dorsal epidermis; e, eye; gl, gland cells; np, nerve plate; o, ovary; ov, ovovitelline duct; pi, sensory pit; ve, ventral epidermis.

sections of a portion behind the head on nine slides; transverse sections of prepharyngeal region on eight slides; sagittal sections of the pharynx on 10 slides; sagittal sections of the copulatory apparatus on 17 slides. NNIBRIV95888 (Field code, 246_2): 380, Cheonpyeong-ri, Sangdong-eup, Yeongwol-gun, Gangwon-do, Republic of Korea; 37°06′34″N, 128°51′29″E; September 29, 2022; coll. J.-H. Song, F. Carbayo, Y. H. Lee and E. J. Ahn; horizontal sections of the cephalic extremity on 12 slides; sagittal sections of the pharynx on nine slides; sagittal sections of the copulatory apparatus on 12 slides. NNIBRIV95889 (Field code, 249_3): 850-5, Waseok-ri, Gimsatgat-myeon, Yeongweol-gun, Gangwon-do, Republic of Korea; 37°05′44″N, 128°36′11″E; September 28, 2022; coll. J.-H. Song, F. Carbayo, Y. H. Lee and E. J. Ahn; preserved in 80% ethanol.

Distribution. Danyang-gun (Chungcheongbuk-do), Mungyeong-si (Gyeongsangbuk-do), and Yeongwol-gun (Gangwon-do) in Republic of Korea.

Type locality. Danyang-gun, Chungcheongbuk-do, Republic of Korea.

Description (external). Living animals are elongate, with a cloak-shaped headplate (Figure 7A,B). At its maximum width, which is 1.3 times the width of the body, the sides of the head are rounded, not recurved. The preserved mature specimens measured 29–52 mm in length, with a body width-to-length ratio of 9%–25%. The mouth of the preserved specimens is located at a distance from the anterior body tip equivalent to 44%–52% of the body length, and the gonopore is located at 58%–69%.

In specimens from Danyang-gun (type locality), the dorsal color of the headplate is sepia brown (RAL 8014; Figure 7A). This color fades toward the sepia brown margins of the headplate, revealing the beige (RAL 1001) ground color. The remaining dorsum is basalt gray (RAL 7012), with five jet black (RAL 9005) longitudinal stripes equally spaced. The median and lateral stripes are 13% of the body width, while the marginal stripes are about 6%. Anteriorly, the median stripe merges with the sepia brown color of the headplate, while the lateral and marginal stripes merge with each other and with the sepia brown margin of the headplate (Figure 7A, C, E). At the posterior body tip, the stripes do not merge. In the paratype NNIBRIV95888, from Cheonpyeong-ri, the ground color is slightly bluish with scattered, faint dark specks lateral to the median stripe, and the lateral and marginal stripes merge, creating a wider band (Figure 7B, G).

The ventral side of the living specimens was not documented. In the preserved specimens, the dorsal color pattern is paler than when alive, and the ventral side is beige in the cephalic

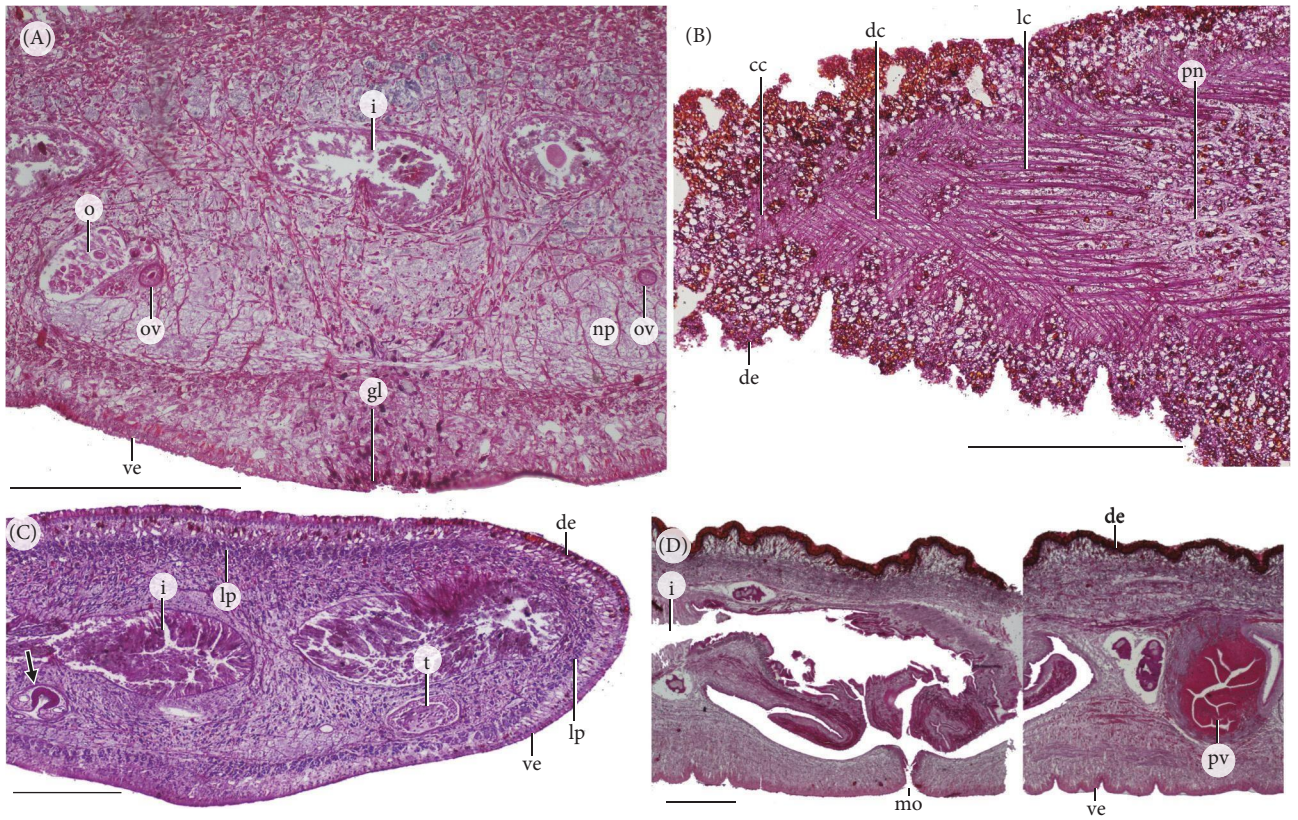

FIGURE 9: *Novibipalium koreanum* sp. nov. Photomicrographs of transverse (A, C), horizontal (B), and sagittal sections of the anterior region (A, B), prepharyngeal region (C), and pharynx of paratypes NNIBRIV93444 (A–C) and NNIBRIV95888 (D). Arrow points to a digenean. Scale bars: 500 µm. cc, circular cutaneous muscle; dc, diagonal cutaneous muscle; de, dorsal epidermis; gl, gland cells; i, intestine; lc, longitudinal cutaneous muscle; lp, longitudinal parenchymal muscle; mo, mouth; o, ovary; ov, ovovitelline duct; pn, peripheral nerve plexus; pv, prostatic vesicle; ve, ventral epidermis.

region, while the margins are darker. In the middle of the ventral surface of the headplate is a whitish, arrow-shaped patch, which extends along the body as a midline about 8%–12% of the body width (Figure 7D, F). This line is bordered along the body by a parasagittal, signal gray (RAL 7004) stripe, which is 8% of the body width. External to this line is a slightly darker paramedian line (9%). The color between the paramedian lines and the body margins is beige. The ventral color of the paratype NNIBRIV95888 follows this pattern but is darker (Figure 7H).

Description (internal). The eyes are 30–40 µm in diameter and are single, cup-shaped. They are arranged in multiple rows that contour the dorsal and ventral margins of the headplate (Figure 7E). Behind the cephalic region, the eyes are sparsely distributed along the body margins. Sensory pits are simple invaginations, 24–50 µm deep (Figure 8A–E). The pits at the front tip are larger and wider (Figure 8D,E) than those on the sides of the headplate. Attached to the deepest portion of the sensory pits at the front tip is a rounded, erythrophil mass, 8–10 µm in diameter, which can also be present in the lumen of the pits (Figure 8B, E). The sensory pits are situated ventromarginally, where small papillae are found, approximately over the anterior half of the headplate.

The width of the creeping sole is 35% of the body width. In the epithelium of the midsagittal sections of the headplate, there is an arrowhead-shaped zone (Figure 7D, F, H), approximately 20% of the headplate width, which is pierced by numerous gland cells producing cyanophil secretion (Figures 8F–G and 9A). Anterior and posterior to this zone are abundant erythrophil glands and scarce xanthophil-type glands. In the prepharyngeal region, rhabditogen cells pierce the epithelium, extending from the dorsolateral region to the ventral side, external to the creeping sole. The creeping sole is pierced by two types of gland cells producing erythrophil and cyanophil secretion, respectively.

The main nervous system consists of a pair of longitudinal nerve cords, which are dilated in the cephalic region to form the cerebral ganglia (Figure 8F). These ganglia are located at a distance from the anterior body tip equivalent to 6% of the body length.

The dorsal cutaneous musculature comprises a subepithelial muscle with very scattered circular fibers, followed by a one-fiber-thick decussate diagonal musculature, and innermost longitudinal muscles in small bundles of 5–12 fibers each (Figure 9B). The ventral cutaneous musculature consists of a very weak layer of circular muscles, followed by a layer of some

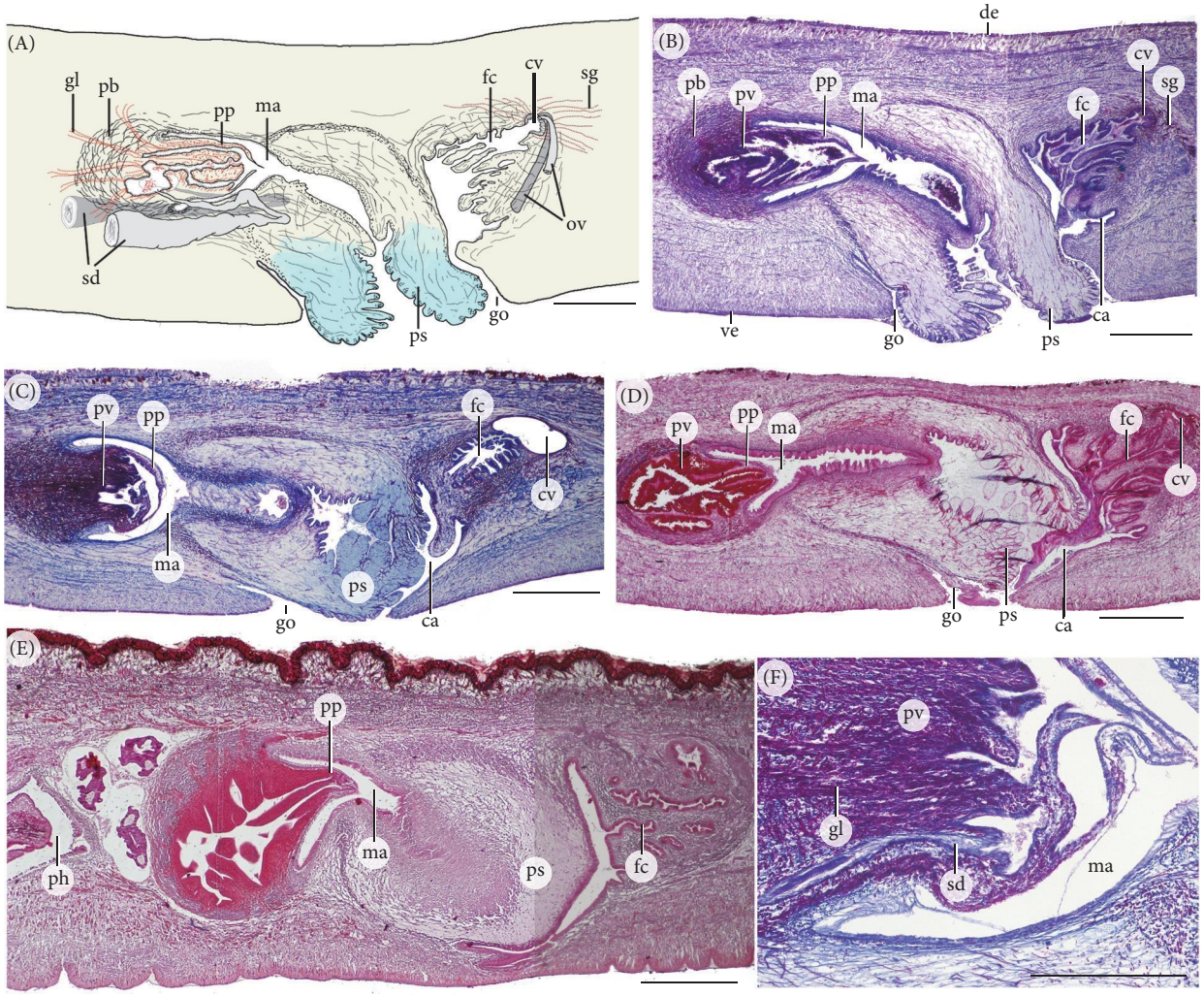

Figure 10: *Novibipalium koreanum* sp. nov. Copulatory apparatus. Diagrammatic reconstruction (A) and photomicrographs of sagittal sections of the copulatory apparatus (B–E) of the holotype (A, B), paratypes NNIBRIV93444 (C, F), NNIBRIV93446 (D), and NNIBRIV95888 (E). Scale bars: 500 μm (A–E) and 250 μm (F). ca, common genial atrium; de, dorsal epidermis; fc, female genital canal; gl, gland cells; go, gonopore; ma, male genital atrium; ov, ovovitelline duct; pb, penis bulb; ph, pharyngeal pouch; pp, penis papilla; ps, pseudophallus; pv, prostatic vesicle; sd, sperm duct; sg, shell glands; ve, ventral epidermis.

decussate diagonal fibers and an innermost layer of longitudinal muscle fibers, the latter gathered in bundles of 4–11 fibers each. CMI: 3.5%–7.0%.

The parenchymal musculature consists of a dorsal muscle of decussate fibers (2.0%–2.6% of the body height), followed by a strong longitudinal muscle (6%–7% of the body height) with bundles of 18–26 fibers each (Figure 9C). This longitudinal muscle is interwoven with diagonal muscle fibers. Between this layer and the intestine is a space with 17% of the body height, bearing longitudinal bundles with 8–15 fibers each, interwoven with diagonal fibers. Beneath the intestine and above the level of the nerve cords is a longitudinal muscle (9%–10%) with fibers organized in bundles of 3–18 fibers each, crossed by transverse fibers. Under the nerve cords is a muscle layer (8%–11%) of diagonal decussate fibers, beneath which is a dense longitudinal muscle (71%–81%) consisting of bundles, each with 18–45 fibers, with diagonal fibers interspersed and oriented in horizontal planes (Figure 9C).

The mouth opens approximately in the middle of the pharyngeal pouch (Figure 9D). The pharynx is collar-shaped, and its length equals that of 98% of the pharyngeal pouch. The outer epithelium of the pharynx is underlain by a one-fiber-thick longitudinal muscle, followed by some scattered circular muscle fibers. The inner pharyngeal epithelium is underlain by a 22–30 μm thick longitudinal muscle, followed by a 25–34 μm thick circular muscle.

The testes are located ventrally, immediately above the main nerve system, and are arranged in a single row on each side of the body (Figure 9C). The anteriormost testes are located immediately behind the ovaries and at a distance from the anterior extremity of the body, equal to 9%–10% of the body length. The posteriormost testes are located lateral to the ventral insertion of the pharynx, and at a distance from the anterior tip of the body equivalent to 36%. The sperm ducts run laterally to the ovovitelline ducts. Lateral to the gonopore, the sperm ducts bend anteriorly to penetrate the lateral aspect of

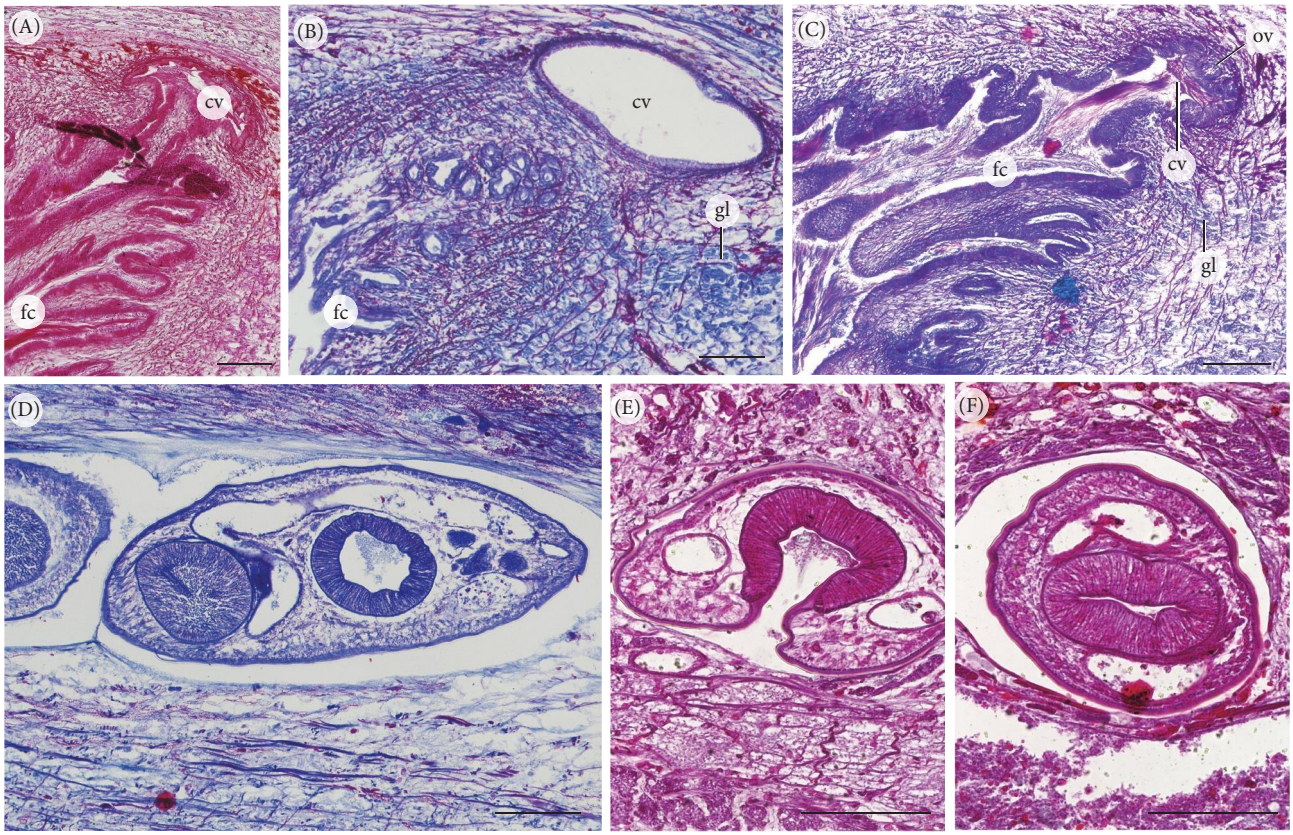

FIGURE 11: *Novibipalium koreanum* sp. nov. Photomicrographs. Sagittal sections of the female genital canal of paratypes NNIBRIV93446 (A), NNIBRIV93444 (B), and holotype (C). D–F digenean found in the parenchyma of paratype NNIBRIV93444. Scale bars: 100 μm. cv, small cavity receiving the ovovitelline ducts; fc:, female genital canal; gl, gland cells; ov, ovovitelline duct.

the penis bulb, within which they run anteriorly to open into lateral pockets of the prostatic vesicle (Figure 10A, F). The point where the sperm ducts open into the prostatic vesicle may be at the base of the penis papilla (Figure 10A) or in the distal portion of this papilla (Figure 10F). The prostatic vesicle is an irregular, plicate cavity occupying a variable portion of the inner space of the penis papilla (Figure 10A–E). The prostatic vesicle opens into the male atrium through a small aperture located at the tip of the penis papilla. This papilla is short and cylindrical, occupying the anterior third of the male atrium.

The sperm ducts are lined with a squamous epithelium. The prostatic vesicle is lined with a squamous-to-cuboidal ciliated epithelium and is pierced by numerous gland cells coming from outside the penis bulb, producing erythrophil granules Figure 10A, E, F). The penis papilla is lined with a columnar, ciliated epithelium around its insertion base and distally by a cuboidal-to-squamous, nonciliated epithelium. A musculature consisting of interwoven circular and longitudinal fibers underlies only the columnar epithelium.

The anterior third of the male atrium is smooth, distally narrowed (Figure 10A–E). The middle third of the male atrium is located within the pseudophallus. This portion of the male atrium is narrow and features small, transverse annular folds; the posteriormost of these may resemble a diaphragm. The posterior third of the male atrium also presents folds and progressively widens toward the tip of the pseudophallus (Figure 10A–D).

The anterior section of the male atrium is lined with a nucleated, ciliated cuboidal epithelium, which is underlain by a circular muscle layer (5 μm thick), followed by a longitudinal muscle layer (9–12 μm thick). The midsection of the male atrium is lined with an infranucleated, nonciliated flat epithelium, which is underlain by a 4 μm thick circular muscle. The distal section of the male atrium is lined with a flat, nonciliated epithelium, which is underlain by scattered circular muscle fibers. The parenchyma of the pseudophallus is occupied by radial and longitudinal muscle fibers and a conspicuous cyanophil mass of granules that do not form strands (Figure 10B–D). The free section of the pseudophallus is lined with a flat epithelium, underlain by a one-fiber-thick circular muscle. The distal portion is underlain by bundles of circular muscles, some of which are apparently radially oriented.

The ovaries are ovoid and measure 260–270 μm in maximum diameter (Figure 9A). They lie immediately above the ventral nerve cords, dorsally to the cerebral ganglia, and at a distance from the anterior end of the body equal to 5.7%–8.3% of the body length. The ovovitelline ducts emerge from the ventrointernal side of the ovaries (Figure 9A). The ovovitelline ducts begin to ascend at the level of the gonopore, and their distal portion may slightly bend anteriorly to open close to each

other into an irregular or ovoid small cavity, ranging between 160–460 μm in maximum diameter (Figures 10A–C and 11A–C).

The ovovitelline ducts are underlain by a 6 μm thick muscle of crisscrossed fibers. The small cavity is lined with a columnar to flat nonciliated epithelium and is pierced by shell glands. The cavity communicates with the posterior or posterodorsal portion of the female genital canal, which is inclined and progressively wider toward the common atrium. The wall of this canal exhibits numerous recesses and folds (Figure 11A–C). The female genital canal is lined with a cuboidal, nonciliated epithelium, which is pierced by gland cells producing fine cyanophil granules and some gland cells producing erythrophil granules. This epithelium is underlain by a 10 μm thick muscle of decussate fibers. A thick and dense muscularis of longitudinal and circular fibers encloses the small cavity and female genital canal (Figure 11A–C).

The gonopore is approximately located midway along the common atrium (Figure 10A–D). This atrium is flattened dorsoventrally and is lined with a cuboidal epithelium. Cilia are present in its anteriormost and posteriormost regions. Some gland cells discharge erythrophil granules through this epithelium, which is surrounded by a 4 μm thick circular muscle.

Remarks. Some digeneans were observed in the parenchyma of the paratype NNIBRIV93444 (Figures 9C and 11D–F).

All adult specimens present a *pseudophallus*, an intromitent organ defined in the diagnosis of *Novibipalium* as "highly muscular male atrium wall which can evert into an elongate penis sheath (pseudophallus), which provided a secondary or distal ejaculatory duct." The animals from Danyang-gun (type locality) are slightly different from the paratype NNIBRIV95888, collected in Yeongwol-gun, 56.8 km straight from the type locality. These differences concern the color of the dorsum and the orientation of the prostatic vesicle. Whereas specimens from Danyang-gun present five longitudinal dorsal stripes, the paratype NNIBRIV95888 exhibits three stripes, with the lateral and marginal stripes apparently merged. Furthermore, the prostatic vesicle of this specimen is dorsoposteriorly inclined (Figure 10E), whereas that of the remaining specimens is horizontal (Figure 10A–D). While one might consider this morphological variation as a reflection of interspecific differences, the molecular delimitation of the species supports their conspecificity [6].

Comparative discussion. Eight species of *Novibipalium* are currently known: *Novibipalium alterifuscatum* Kawakatsu et al., 1998, *Novibipalium falsifuscatum* Kawakatsu et al., 1998, *Novibipalium miyukiae* Kawakatsu et al., 2005, *Novibipalium murayamai* Kawakatsu et al., 2005, *Novibipalium pseudophallicum* (de Beauchamp, 1925), *Novibipalium rhynchophorum* Solà and Sluys, 2023, *Novibipalium trifuscostriatum* (Kaburaki, 1922), and *Novibipalium venosum* (Kaburaki, 1922). The external appearance of the new species differs readily from the congeneric species, as the only two *Novibipalium* species with dorsal longitudinal stripes present either two (*N. pseudophallicum*) or three (*N. trifuscostriatum*) stripes, whereas *N. koreanum* sp. nov. displays a maximum of five stripes.

Regarding the copulatory apparatus, *Novibipalium koreanum* sp. nov. differs from *N. miyukiae* and *N. murayamai* in that the shell glands open along almost the entire epithelium of the female genital canal in these two species, whereas only the anterior, proximal portion of the female genital canal receives shell glands in *N. koreanum* sp. nov. Among the remaining species, *N. alterifuscatum*, *N. falsifuscatum*, *N. pseudophallicum*, *N. trifuscostriatum*, and *N. venosum* have the female genital canal vertically located, in contrast to that of the new species, which is inclined at approximately 45°. In these features, *N. rhynchophorum* is similar to the new species. However, it can be differentiated from the new species in that the penis papilla in the former is located beneath the penis bulb, whereas the penis bulb in *N. koreanum* sp. nov. is situated anterior to the penis papilla. Furthermore, in *N. rhynchophorum*, the sperm ducts run dorsally to the penis papilla, while they run ventrally in the new species.

3.2. Phylogenetic Analysis. All phylogenetic analyses retrieved the two new species as robustly supported monophyletic groups, while *Bipalium* was found to be polyphyletic (Figure 12; Figures S1–S3). The phylogenetic trees inferred from the concatenated dataset (Figure 12), the 18S single-gene dataset (Figure S1), and the 28S single-gene dataset (Figure S2), all support the clade *B. gwangneungensis* sp. nov. + *B. adventitium* and the clade *N. koreanum* sp. nov. + remaining *Novibipalium* species (SH-aLRT ≥80%, UFBoot ≥95%). Meanwhile, the COI single-gene tree (Figure S3), shows a sister relationship between *B. gwangneungensis* sp. nov. and the *N. koreanum* sp. nov. + *N. venosum* clade, but the node connecting these two clades is not supported.

The genus *Bipalium* was retrieved as polyphyletic in all analyses, with its members found as sister to species of *Vermiviatum* or *Diversibipalium*. Nothing further can be added regarding the collective genus *Diversibipalium*, as it encompasses species that are poorly known from a morphological perspective.

4. General Discussion

The congruence between the morphological and molecular data provides strong evidence for the robustness of the proposal of the two new species. Given the geographic location of Korea in East Asia, it is not surprising that the two new species are members of *Bipaliinae*. As observed by Solà et al. [3], *Bipalium* was retrieved as polyphyletic, but no taxonomic action was taken to split the genus into several genera due to the paucity of data available on its members.

Prior to this work, *Microplana unilineata* and *Diversibipalium koreense* were the only land planarians known from the Republic of Korea. However, their exact type localities remain uncertain, and no subsequent confirmed records of these species have been documented, making their current status questionable and in need of verification. These species were presumably collected on Jeju Island (also called Quelpart), as proposed by Ogren and Kawakatsu [21] based on indirect evidence. This island is situated off the southern coast of the Korean Peninsula, whose native biota is mostly derived from continental Asia [22].

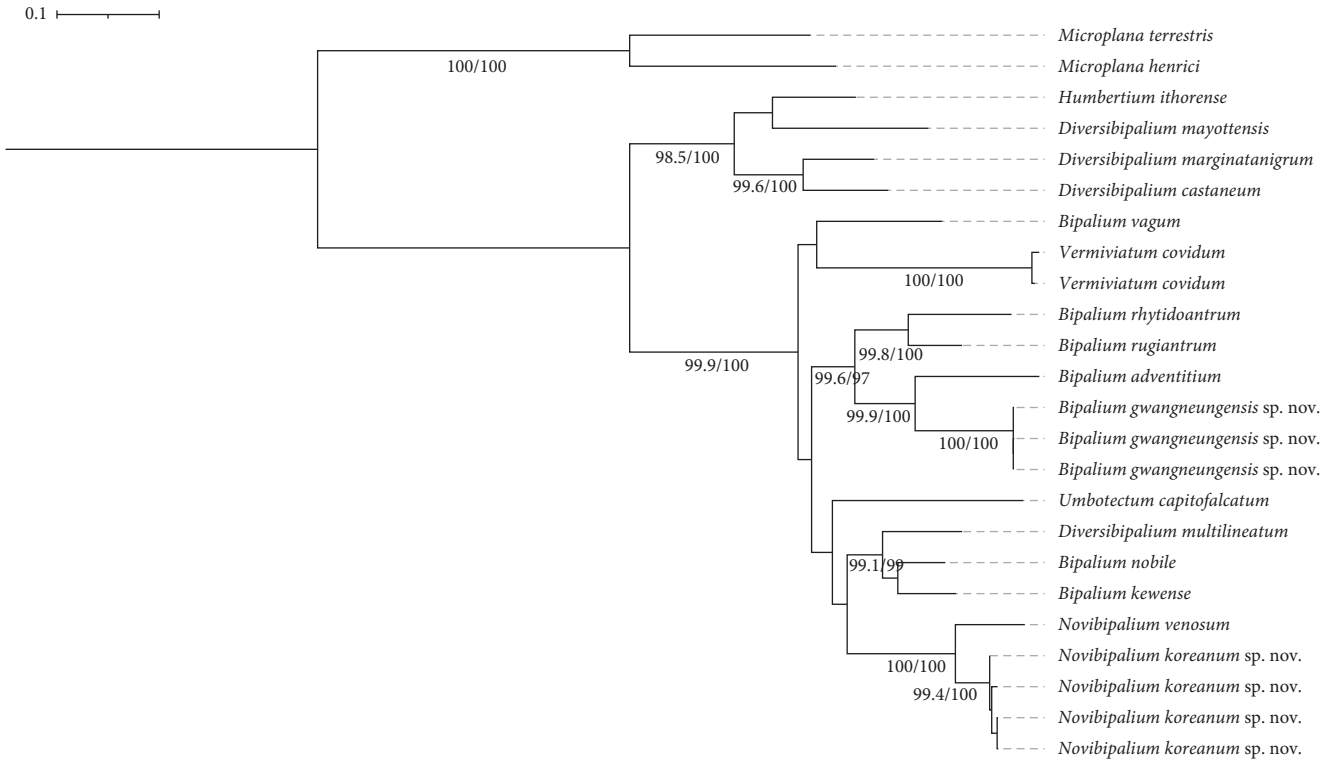

Figure 12: Phylogenetic tree inferred from the three concatenated genes (18S rDNA, 28S rDNA, and COI) using maximum likelihood as the optimality criterion. Numbers at the nodes correspond to SH-aLRT (%) and ultrafast bootstrap support (%). Only support values above SH-aLRT ≥80% and UFBoot ≥95% are shown. Scale bar represents number of substitutions per site.

The Korean Peninsula underwent large-scale overexploitation and deforestation during the latter period of Japanese occupation (1910–1945) and the civil war (1950–1953), and only 0.4% of the current vegetation remains in a fully natural state, mainly as forests and alpine meadows [23]. As a result, many soil invertebrate species, including land planarians, must have vanished following deforestation. Winsor [24, 25] highlighted the importance of small pockets of remnant forest for the conservation of land planarians. On the one hand, the persistence of small forest pockets in Korea until the present day [26–28] may explain the high number of land planarian species recently discovered across the country [6]. On the other hand, the fact that virtually all of these species remain undescribed may be related to a lack of local taxonomic specialists in platyhelminths [29]. Hopefully, this contribution and our collaborative research will help change this situation.

5. Conclusion

This study provides compelling evidence for the recognition of two new Bipaliinae species in Korea through an integrative taxonomic approach that combines morphological traits and molecular phylogenetics. As the first formal taxonomic work on Korean land planarians in a century, our research not only fills a critical gap in the faunal records of the region but also highlights the need to address overlooked components of Korea's invertebrate fauna. Continued taxonomic efforts, bolstered by international collaboration, are essential to uncover and document the full extent of Korea's land planarian fauna.

Beyond its immediate taxonomic contributions, this study also underscores the broader ecological and historical context in which Korea's land planarian diversity is situated. The drastic deforestation and land-use changes in the 20th century, particularly during the Japanese occupation and Korean War, likely led to the decline or disappearance of many soil-dwelling invertebrates, including land planarians. Yet, the persistence of small, remnant forest patches across the Korean Peninsula appears to have served as important refuges, supporting the survival of some land planarian species despite widespread habitat loss. By bringing to light part of a long-overlooked invertebrate lineage, our research emphasizes the importance of taxonomy in biodiversity science and the need to protect vulnerable habitats that support overlooked soil-dwelling species.

Data Availability Statement

The authors declare that the data supporting the findings of this study are available within the article and its supporting information (Figures S1–S3). Should any raw data files be needed in another format, they are available from the corresponding author upon reasonable request. The sequences have been deposited in GenBank (accession numbers: PQ652198–PQ652204 for 18S rDNA, PQ652205–PQ652211 for 28S rDNA, and PQ653970–PQ653976 for COI mtDNA). The new taxa have been registered in ZooBank (urn:lsid:zoobank.org:act:E8242AF9-B013-49FF-8C9E-925C9F6FEB85 for *Bipalium gwangneungensis* sp. nov., and urn:lsid:zoobank.org:act:

BAF2EE11-A220-4938-B927-AC97186AC024 for *Novibipalium koreanum* sp. nov.).

Ethics Statement

The authors have nothing to report.

Disclosure

Both authors read and approved the final manuscript.

Conflicts of Interest

The authors declare no conflicts of interest.

Author Contributions

Both authors contributed to the study's conception, design, and writing. Fernando Carbayo conducted the morphological analyses, and Ji-Hun Song carried out the molecular analyses.

Funding

This work was supported by a grant from the Nakdonggang National Institute of Biological Resources (NNIBR), funded by the Ministry of Environment (MOE) of the Republic of Korea (Grant NNIBR20251101) and São Paulo Research Foundation-FAPESP (Grant 2022/11972-2).

Acknowledgments

We thank Jin-Young Kim, Eun Jung Ahn, Gwiae Kim, Yeoung Hee Lee (NNIBR), and Ah Yeoung Kim (KNA, Korea National Arboretum) for helping with collecting specimens in this study; KNA for licensing the field work in Gwangneung Forest. Geison Castro and Lucas Beltrami (USP) helped with histological processing.

Supporting Information

Additional supporting information can be found online in the Supporting Information section. (*Supporting Information*) Figure S1. Phylogenetic tree inferred from the 18S rDNA using maximum likelihood as the optimality criterion. Numbers at the nodes correspond to SH-aLRT (%) and ultrafast bootstrap support (%). Only support values above SH-aLRT ≥80% and UFBoot ≥95% are shown. Scale bar represents the number of substitutions per site. Figure S2. Phylogenetic tree inferred from the 28S rDNA using maximum likelihood as the optimality criterion. Numbers at the nodes correspond to SH-aLRT (%) and ultrafast bootstrap support (%). Only support values above SH-aLRT ≥80% and UFBoot ≥95% are shown. Scale bar represents the number of substitutions per site. Figure S3. Phylogenetic tree inferred from the COI mtDNA using maximum likelihood as the optimality criterion. Numbers at the nodes correspond to SH-aLRT (%) and ultrafast bootstrap support (%). Only support values above SH-aLRT ≥80% and UFBoot ≥95% are shown. Scale bar represents the number of substitutions per site.

References

[1] National Institute of Biological Resources (NIBR), "National List of Korea. National Institute of Biological Resources," 2023, Accessed April 8, 2025 https://kbr.go.kr.

[2] W. Stimpson, "Prodromus Descriptionis Animalium Evertebratorum, Quae in Expeditione ad Oceanum, Pacificum Septentrionalem a Republica Federata Missa, Johanne Rodgers Duce, Observavit et Descripsit," in *Proceedings of the Academy of Natural Sciences of Philadelphia*, 9, (Academy of Natural Sciences of Philadelphia, 1857): 19–31.

[3] E. Solà, R. Sluys, M. Riutort, and M. Kawakatsu, "Molecular Phylogenetics Facilitates the First Historical Biogeographic Analysis of the Hammerhead Worms (Platyhelminthes: Tricladida: Bipaliinae), With the Description of Twelve New Species and Two New Genera," *Zootaxa* 5335, no. 1 (2023): 1–77.

[4] R. E. Ogren, M. Kawakatsu, and E. M. Froehlich, "Additions and Corrections of the Previous Land Planarian Indices of the World (Turbellaria, Tricladida, Terricola)," *Bulletin of Fuji Women's College* 30, no. 2 (1992): 59–103.

[5] L. Winsor, "A Revision of the Cosmopolitan Land Planarian, *Bipalium kewense*, Moseley, 1878 (Turbellaria: Tricladida: Terricola)," *Zoological Journal of the Linnaean Society* 79, no. 1 (1983): 61–100.

[6] J.-H. Song and F. Carbayo, "Present and Future of the Study on Korean Land Planarians (Platyhelminthes: Tricladida: Geoplanidae)," *Zoologia (Curitiba)* 41 (2024): e23083.

[7] D. P. Shorthouse, "SimpleMappr, An Online Tool to Produce Publication-Quality Point Maps," 2010, http://www.simplemappr.net.

[8] J. E. Cason, "A Rapid One-Step Mallory-Heidenhain Stain for Connective Tissue," *Stain Technology* 25, no. 4 (1950): 225-226.

[9] E. M. Froehlich, "Sôbre Espécies Brasileiras Do gênero Geoplana," *Boletim Da Faculdade De Filosofia, Ciências e Letras Da Universidade De São Paulo, Série Zoologia* 19 (1955): 289–369.

[10] M. Álvarez-Presas, F. Carbayo, J. Rozas, and M. Riutort, "Land Planarians (Platyhelminthes) as a Model Organism for Fine-Scale Phylogeographic Studies: Understanding Patterns of Biodiversity in the Brazilian Atlantic Forest Hotspot," *Journal of Evolutionary Biology* 24, no. 4 (2011): 887–896.

[11] P. Sunnucks, M. J. Blacket, J. M. Taylor, et al., "A Tale of Two Flatties: Different Responses of Two Terrestrial Flatworms to Past Environmental Climatic Fluctuations at Tallaganda in Montane Southeastern Australia," *Molecular Ecology* 15, no. 14 (2006): 4513–4531.

[12] S. Carranza, G. Giribet, C. Ribera, and M. Riutort, "Evidence That Two Types of 18S rDNA Coexist in the Genome of *Dugesia* (Schmidtea) Mediterranea (Platyhelminthes, Turbellaria, Tricladida)," *Molecular Biology and Evolution* 13, no. 6 (1996): 824–832.

[13] M. Álvarez-Presas, J. Baguñà, and M. Riutort, "Molecular Phylogeny of Land and Freshwater Planarians (Tricladida, Platyhelminthes): From Freshwater to Land and Back," *Molecular Phylogenetics and Evolution* 47, no. 2 (2008): 555–568.

[14] M. Kearse, R. Moir, A. Wilson, et al., "Geneious Basic: An Integrated and Extendable Desktop Software Platform for the Organization and Analysis of Sequence Data," *Bioinformatics* 28, no. 12 (2012): 1647–1649.

[15] J. Trifinopoulos, L.-T. Nguyen, A. von Haeseler, and B. Q. Minh, "W-IQ-TREE: A Fast Online Phylogenetic Tool for Maximum Likelihood Analysis," *Nucleic Acids Research* 44, no. W1 (2016): W232–W235.

[16] S. Guindon, J.-F. Dufayard, V. Lefort, M. Anisimova, W. Hordijk, and O. Gascuel, "New Algorithms and Methods to Estimate Maximum-Likelihood Phylogenies: Assessing the Performance of PhyML 3.0," *Systematic Biology* 59, no. 3 (2010): 307–321.
[17] B. Q. Minh, M. A. T. Nguyen, and A. von Haeseler, "Ultrafast Approximation for Phylogenetic Bootstrap," *Molecular Biology and Evolution* 30, no. 5 (2013): 1188–1195.
[18] I. Letunic and P. Bork, "Interactive Tree of Life (iTOL) v6: Recent Updates to the Phylogenetic Tree Display and Annotation Tool," *Nucleic Acids Research* 52, no. W1 (2024): W78–W82.
[19] Y. C. Cho, H. C. Shin, S. S. Kim, and C. S. Lee, "Dynamics and Conservation of the Gwangneung National Forest in Central Korea: A National Model for Forest Restoration," *Journal of Plant Biology* 50, no. 6 (2007): 615–625.
[20] P. de Beauchamp, "Planaires Terrestres De l'Indochine Française Récoltées Par M. C. Dawydoff," *Mémoires Du Muséum National d'Histoire Naturelle, Nouvelle Série* 10 (1939): 299–338.
[21] R. E. Ogren and M. Kawakatsu, "Index to the Species of the Genus *Bipalium* (Turbellaria, Tricladida, Terricola)," *Bulletin of Fuji Women's College* 25, no. 2 (1987): 79–119.
[22] J. R. Ali, "Islands as Biological Substrates: Continental," *Journal of Biogeography* 45, no. 5 (2018): 1003–1018.
[23] B. S. Choi, "Nature in Korea," in *The Biodiversity and Protected Areas of Korea*, ed. H. Y. Heo, (Ministry of Environment and Korea National Park Service, 2007).
[24] L. Winsor, "The Biodiversity of Terrestrial Flatworms (Tricladida: Terricola) in Queensland: A Preliminary Report," *Memoirs of the Museum of Victoria* 56, no. 2 (1997): 575–579.
[25] L. Winsor, "The Australian Terrestrial Flatworm Fauna (Tricladida: Terricola)," *Pedobiologia* 42, no. 5-6 (1998): 457–463.
[26] W. Kang, J. Kim, C.-R. Park, and J. H. Sung, "Comparing Connectivity in Forest Networks of Seven Metropolitan Cities of South Korea," *Korean Journal of Agricultural and Forest Meteorology* 16, no. 2 (2014): 93–102.
[27] J. Kwon, J. H. Oh, J. Y. Lee, C. R. Park, and M. S. Choi, "Locations and Topographical Character of the Maeulsoop in the Southwestern and the Eastern Region," *Journal of the Korean Association of Geographic Information Studies* 11, no. 4 (2008): 85–93.
[28] M. J. Park, S. B. Kim, C. S. Jang, M. J. Shin, and E. J. Kim, "A Study on the Analysis of Location on the Traditional Rural Village Forest in South Korea," *Journal of Korean Society of Rural Planning* 19, no. 1 (2013): 149–164.
[29] J. Lim, J. Bhak, and W.-K. Paek, "Current Status and the Future of Korean Biodiversity," *Journal of Korean Nature* 1, no. 2 (2008): 231–235.